Journal of Earth Science, *Vol. 29*, *No. 2*, *p. 441–451*, *April 2018* *ISSN 1674-487X*
Printed in China
https://doi.org/10.1007/s12583-017-0937-z

New Progress in Paleoearthquake Studies of the East Sertengshan Piedmont Fault, Inner Mongolia, China

Zhongtai He*[1], Baoqi Ma[1], Jianyu Long[1], Jinyan Wang[2], Hao Zhang[1]
1. *Key Laboratory of Crustal Dynamics*, *Institute of Crustal Dynamics*, *China Earthquake Administration*, *Beijing* 100085, *China*
2. *Institute of Earthquake Engineering for Jiangsu Province*, *Nanjing* 210014, *China*
Zhongtai He: https://orcid.org/0000-0001-5436-5759

ABSTRACT: The two eastern segments of the Sertengshan piedmont fault have moved considerably since the Holocene. Several paleoseismic events have occurred along the fault since 30 ka BP. Paleoearthquake studies have been advanced by digging new trenches and combining the results with the findings of previous studies. Comprehensive analyses of the trenches revealed that 6 paleoseismic events have occurred on the Kuoluebulong segment since approximately 30 ka BP within the following successive time periods: 19.01–37.56, 18.73, 15.03–15.86, 10.96, 5.77–6.48, and 2.32 ka BP. The analyses also revealed that 6 paleoseismic events have occurred on the Dashetai segment since approximately 30 ka BP, and the successive occurrence times are 29.07, 19.12–28.23, 13.92–15.22, 9.38–9.83, 6.08–8.36, and 3.59 ka BP. The results indicate that quasi-periodic recurrences occurred along the two segments with an approximate 4 000 a mean recurrence interval. The consistent timing of the 6 events between the two segments indicates that the segments might conform to the cascade rupturing model between the two segments. As recorded by a large number of Chinese historical texts, the latest event on the Kuoluebulong segment is the historical *M* 8.0 earthquake occurred on November 11, 7 BC.
KEY WORDS: active fault, Sertengshan piedmont fault, fault segmentation, paleoearthquake.

0 INTRODUCTION

The Ordos Block is a unique uplifted region that contains little interior deformation. The extensional Shanxi and the Yinchuan-Jilantai basins, characterized by right-lateral shear, lie on the eastern and western sides of the Ordos Block, respectively. The extensional Weihe and Hetao basins, characterized by left-lateral shear, lie on the southern and northern sides of the Ordos Block, respectively. Transpressional left-lateral arcuate faults are located along the southwestern side of the Ordos Block. The Hetao Basin is located between the Ordos Block and the Yinshan Mountains. The basin is bounded to the west by the Langshan fault and to the east by the Helingeer fault. The northern margin of the basin is marked by the Sertengshan piedmont fault, Wulashan piedmont fault and Daqingshan piedmont fault, and the southern margin of the basin is marked by the northern margin fault of the Ordos Block. The Hetao Basin is oriented in an E-W direction and is 440 km long E-W and 40–80 km wide N-S. The maximum thickness of the Cenozoic and Quaternary strata are 12 000 and 2 400 m, respectively, in the western part of the basin (Fig. 1a; Du et al., 2016; Jiang et al., 2014; Research Group on 'Active Fault System around Ordos Massif', SSB, 1988).

*Corresponding author: hezhongtai@126.com

Manuscript received October 25, 2016.
Manuscript accepted July 15, 2017.

The Sertengshan piedmont fault is approximately 190 km in length and lies in Inner Mongolia in northern China, starting from Dongwugai and progressing in the E-W direction through Langshankou, Wujiahe, to Wubulangkou, and it then turns 300° and proceeds through Dongfengcun, Dashetai, Wulancun to Tailiang at the end (Fig. 1b). This fault is in the EW and SE directions and trends southward as a typical normal dip-slip fault. Together with the Wulashan and Daqingshan faults (F2, F3 in Fig. 1a) to the east, it is part of the northern fracture zone of the Hetao Basin and controls the basin's formation and development (Fig. 1a). The *M* 6.0 Wuyuan historical earthquake in 1934 and the *M* 6.0 Wuyuan historical earthquake in 1979 occurred in this fault. More than 10 trenches have been dug along the fault to study its paleoearthquakes (Chen et al., 2003a, b; Yang et al., 2003, 2002; Wu et al., 1996; Research Group on 'Active Fault System around Ordos Massif', SSB, 1988). However, most of the trenches are located in the western part of the fault to the west of Wubulangkou, and only 3 trenches are located in the eastern part of the fault, which is approximately 90 km to the east of Wubulangkou. We have dug 3 new trenches on the east fault to the east of Wubulangkou to study the paleoearthquakes of the east segments of the fault. This paper comprehensively analyzes the results from previous trenches and our 3 new trenches and provides new insights into the paleoearthquakes of the east Sertengshan piedmont fault.

1 FAULT SEGMENTATION

The critical step in fault segmentation is to determine the boundaries between adjacent fault segments, which are the

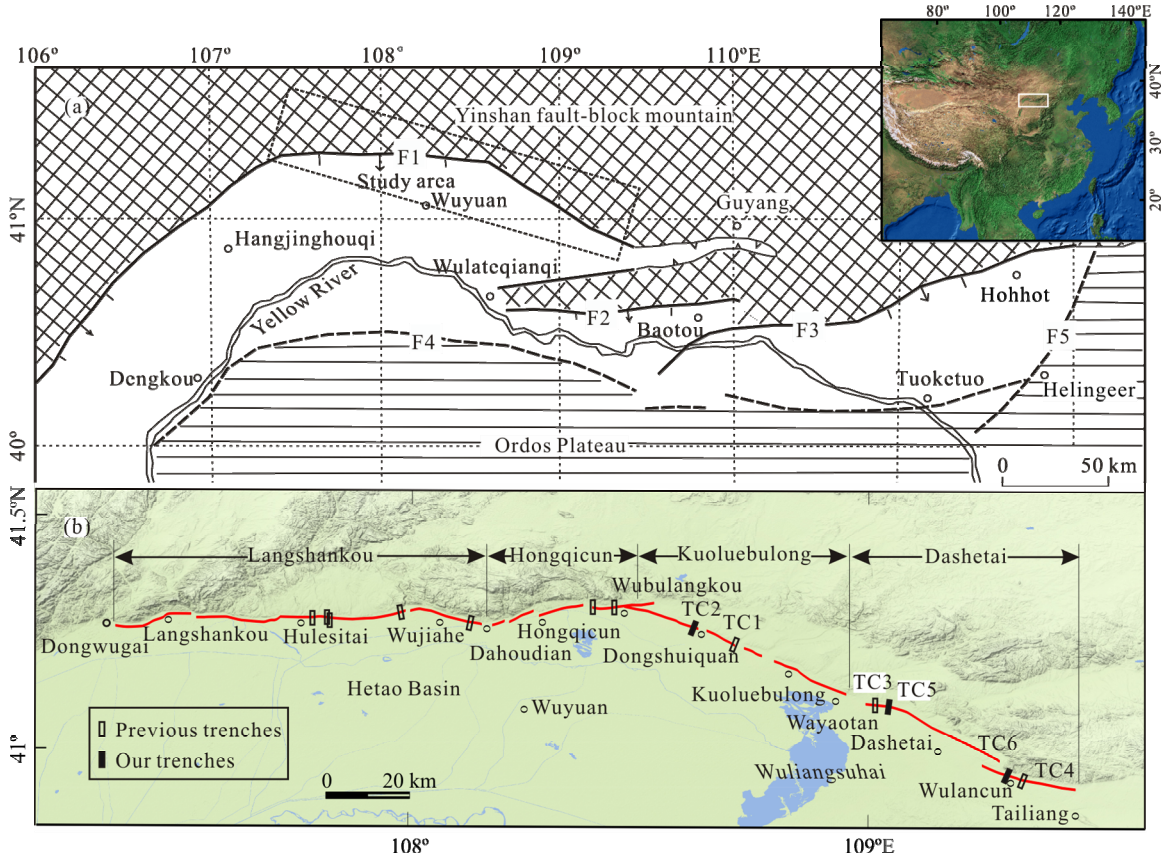

Figure 1. Distribution of the Sertengshan piedmont fault. F1. Sertengshan piedmont fault; F2. Wulashan fault; F3. Daqingshan piedmont fault; F4. the northern margin fault of the Ordos Plateau; F5. Helingeer fault.

rupture endpoints of the fault segments (Wheeler, 1989). Researchers have studied fault segmentation in China mainland and concluded that the boundaries between normal faults in China mainland can be characterized as bedrock bulge, oblique stepover, buried bedrock ridge, fault gap zone and T-vertex (Zhang et al., 1998; Deng and Zhang, 1995; Zhang and Deng, 1995; Ding et al., 1993).

The Sertengshan piedmont fault is divided into 2 segments at the boundary of Wubulangkou (Wu et al., 1996) and is divided into the following 4 segments at the boundaries of the Dahoudian spur, the Delingshan spur and the Xiaoshetaioblique stepover: Wujiahe segment (Dongwugai-Dahoudian), Dongfengcun segment (Dahoudian-Delingshan), Dashetai segment (Delingshan-Xiaoshetai), and Wulancun segment (Xiaoshetai-Tailiang).

Field investigations have suggested differences in the fault's geometric distribution between the west fault and east fault of Wubulangkou. The fault lies in an EW direction west of Wubulangkou and at 300° east of Wubulangkou. Wu et al. (1996) divided the fault into 2 segments with Wubulangkou representing the boundary. Chen et al. (2003a) regarded the two sides of Wubulangkou as a single arcual fault in the NE direction.

Based on field investigations and measurements of the Sertengshan piedmont fault from Dahoudian to Wayaotan, we concluded that the segment is not a single arcual fault in the NE direction and considered it to be divided into 2 secondary segments: east-trending Hongqicun segment (Dahoudian-Wubulangkou) and southeast-trending Kuluebulong segment (Wubulangkou-Wayaotan), and a T-shaped junction is observed between the two segments.

We acquired 203 terrace heights using a laser distance meter and acquired the terrain data of typical structural landforms using the RTK (real time kinematic) measuring method along the fault (Fig. 2). We define the levels of terraces in different segments along the fault based on the terrace heights and the terrace deposits. The T1 terraces are several meters to ten meters high, and are composed of variegated alluvial gravels. There are several faults in the front margin of the T1 terraces. The T2 terraces are ten meters to more than 20 m high, and are composed of 0.2–2 m thick variegated alluvial gravels on top and yellow-green lacustrine deposits at bottom. There are several faults in the front margin of the T2 terraces. The T3 terraces are 20 m to more than 30 m high, and have the similar deposits with the T2 terraces. There are not faults in the front margin of the T3 terraces.

We also collected geological borehole data on the basin stratigraphy in the hanging wall. Using these data, we obtained the absolute vertical displacement of the fault. We performed optically stimulated luminescence (OSL) dating on samples from the terraces on the footwall and identified the stratigraphic ages of the units in the geological boreholes in the hanging wall to calculate the absolute vertical slip rates of the Sertengshan piedmont fault. We combine the vertical slip rates and the tectonic geomorphologic features of the different segments of the fault to identify differences in fault activity among the segments of the fault. The results indicate that the mean vertical slip rates are 1.75 in Fanrong, 1.45 in Fengyu, 1.58 in

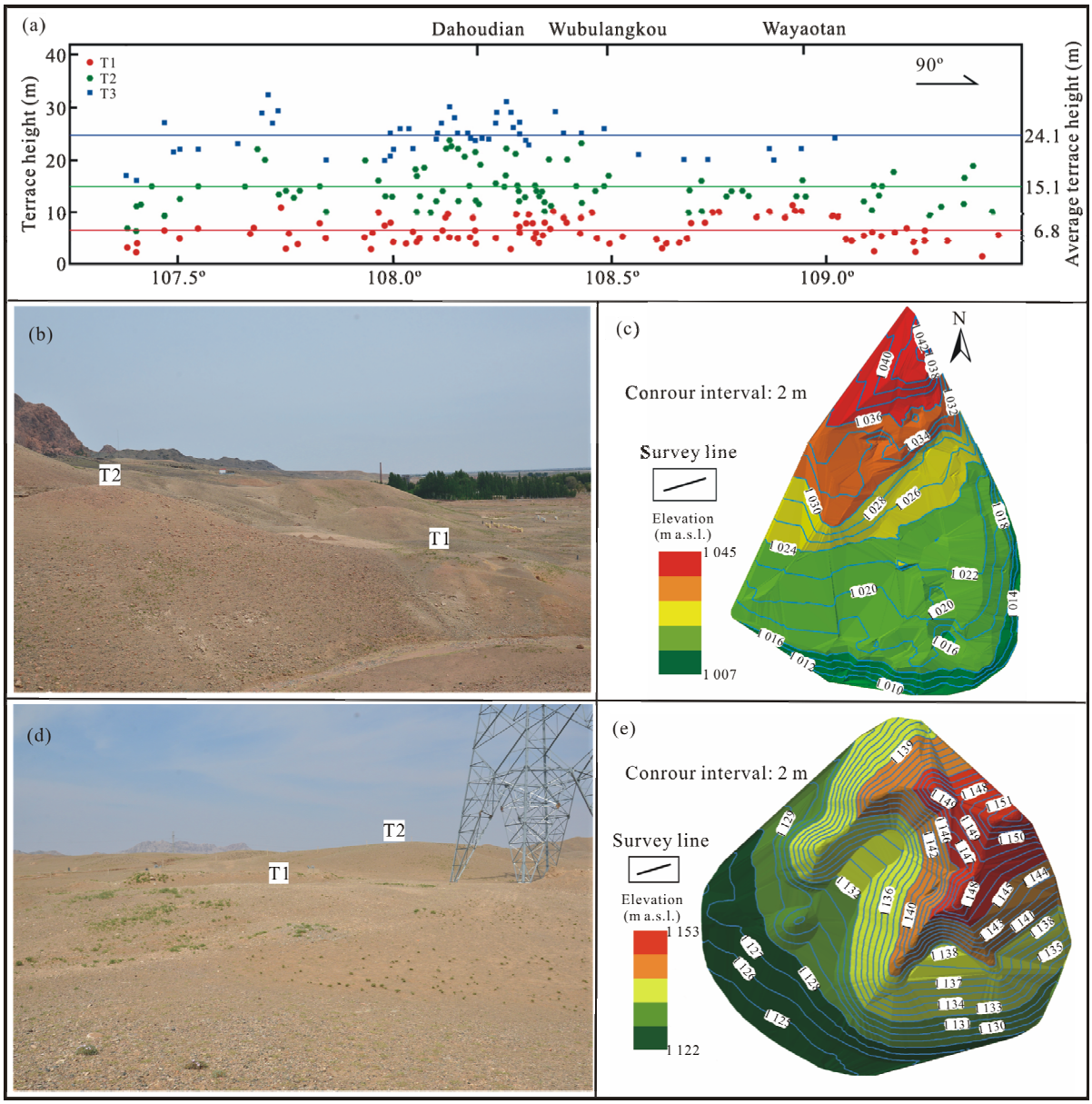

Figure 2. The terraces height distribution and geomorphology of the Sertengshan piedmont. (a) Terraces height distribution; (b) terrace geomorphology of Wujiahe site (view to the E); (c) DEM map of Wujiahe site; (d) terrace geomorphology of Dashetai site (view to the E); (e) DEM map of Dashetai site.

Tongyilong, 1.81 in Wujiahe, 1.66 Hongqicun, 0.98 in Wubulangkou, 0.89 in Delingshan, 0.94 in Xishuiquan, and 0.74 mm/a in Kuoluebulong since 65.0±3.2 ka BP. The mean vertical slip rates of the fault during the Holocene are 2.05 in Fanrong, 1.72 in Fengyu, 0.86 in Wubulangkou, 2.13 in Delingshan, 1.42 in Xishuiquan, and 2.07 mm/a in Kuoluebulong.

Based on the characteristics of the geometrical distribution, the tectonic activity and geomorphological features, paleoearthquakes and segment boundary features of the Sertengshan piedmont fault, we divided the fault into 4 segments: the Langshankou (Dongwugai-Wayaotan) and Hongqicun segments (Dahoudian-Wubulangkou) in the EW direction and the Kuoluebulong (Wubulangkou-Wayaotan) and Dashetai segments (Wayaotan-Tailiang) in the NW direction (Fig. 1b).

The Langshankou segment is 75 km long in the EW direction and is composed of left-stepped, oblique-arranged faults in the Langshankou area; it is linear in the Hulesitai area and composed of right-stepped, oblique-arranged faults in the Wujiahe area, and it ends in a southward mountain spur in Dahoudian. The Hongqicun segment is 25 km long in the EW direction and consists of right-stepped, oblique-arranged subfractures. The subfractures are short in length. The boundary between the Langshankou and Hongqicun segments is the southward Dahoudian Mountain spur, which is a bedrock bulge forming a permanent segment boundary. The Kuolunbulong segment is 45 km long in the NW direction and composed of several secondary faults that are arranged end to end in a line and mostly arcual faults in the NE direction. The Dashetai segment is approximately 45 km long in the NW direction, and it is composed of two secondary faults which are right-stepped, oblique-arranged in the Xiaoshetai area. The fault in the Dashetai area is arcual in the NE direction. The fault between

Wulancun and Tailiang is straight in the WNW direction. The boundary between the Kuoluebulong and Dashetai segments is the Delingshan Mountain spur toward the SW.

2 TRENCHES—PALEOEARTHQUAKE ANALYSES

Previous researchers dug 10 trenches on the Sertengshan piedmont fault to study the paleoearthquakes in the region (Fig. 1b), and only 3 of these trenches were located on the Kuoluebulong and Dashetai segments, although these trenches did not expose recent strata. We dug 3 more trenches on the two segments to complete the paleoearthquake study. The 3 new trenches revealed evidence of Holocene paleoseismic events that occurred on the two segments.

We analyzed 40 samples with OSL at the Key Laboratory of Crustal Dynamics, Institute of Crustal Dynamics, China Earthquake Administration, Beijing. For each sample, the middle part of the sample, which was not disturbed, was used for measurement. We dried and ground 20 g of the sample to measure the content of U, Th and K. We added hydrogen peroxide and hydrochloric acid to the remaining sample to remove the carbonates and organic matter. We then isolated the particle groups from 4 to 11 μm using the hydrostatic settlement method. We treated the particle groups with fluorosilicate to obtain fine-grained quartz for further measurement. An equal dose (*DE*) of the sample was determined using a Risoe DA-20-C/D OSL auto-measuring system. The natural OSL dose is measured via the middle-grain single-aliquot regenerative-dose (SAR) method. The U, Th and K contents in the environmental dose rate (*D*) is measured with an ELEMENT inductively coupled plasma mass spectrometer. Finally, the sample's age is determined according the equation age (*A*)=equal dose (*DE*)/environmental dose rate (*D*) (Nulay et al., 2016; Lu et al., 2007; Murray and Wintle, 2003, 2000; Aitken, 1998). Twenty-one samples are reasonable and their dating results are used in the paper (Table 1). The result of 21 540±80 a is getting from the ^{14}C method.

2.1 Dongshuiquan Trench (TC2)

The Dongshuiquan trench is located on the front margin of T1, which is approximately 7.8 m high. The trench is 16 m in length, 5 m in width and 7 m in depth (Figs. 3a and 3b). Both the

Table 1 Ages of the trenches on the east Sertengshan piedmont fault

Sample location	Field number	U (μg/g)	Th (μg/g)	K (wt.%)	Environmental dose rate (Gy/ka)	Equivalent dose (Gy)	Age (ka BP)
Dongshuiquan trench	DSQ-OSL-01	1.69	8.48	1.72	3.43	7.95±0.59	2.32±0.29
Dongshuiquan trench	DSQ-OSL-03	0.86	3.43	2.37	3.27	19.17±1.20	5.86±0.69
Dongshuiquan trench	DSQ-OSL-04	0.67	4.16	2.38	3.29	112.61±4.83	34.26±3.73
Dongshuiquan trench	DSQ-OSL-05	1.18	4.49	1.96	3.08	58.51±3.34	19.01±2.19
Dongshuiquan trench	DSQ-OSL-06	0.45	1.61	1.94	2.49	128.20±13.12	51.45±7.36
Dongshuiquan trench	DSQ-OSL-07	1.17	5.12	1.57	2.73	21.29±2.03	7.79±1.08
Dongshuiquan trench	DSQ-OSL-08	1.57	4.06	1.88	3.09	57.84±2.57	18.73±2.05
Dongshuiquan trench	DSQ-OSL-10	2.12	5.29	2.14	3.69	55.54±6.31	15.03±2.28
Dongshuiquan trench	DSQ-OSL-11	1.18	2.96	1.93	2.89	30.06±1.34	10.39±1.14
Dongshuiquan trench	DSQ-OSL-12	1.35	4.93	1.97	3.19	20.68±1.45	6.48±0.79
Mabozi trench	MBZ-OSL-01	1.86	8.97	1.63	3.45	100.19±8.71	29.07±3.85
Mabozi trench	MBZ-OSL-02	2.11	12.80	1.64	3.95	15.42±0.93	3.90±0.46
Mabozi trench	MBZ-OSL-03	2.17	8.10	1.78	3.62	298.98±22.28	82.49±10.29
Mabozi trench	MBZ-OSL-04	2.10	10.40	2.07	4.14	248.14±18.04	59.93±7.41
Mabozi trench	MBZ-OSL-07	1.96	18.60	1.83	4.69	183.30±12.82	39.06±4.77
Mabozi trench	MBZ-OSL-08	1.88	13.40	1.68	3.97	315.81±33.21	79.62±11.56
Mabozi trench	MBZ-OSL-09	2.47	8.47	1.53	3.52	67.07±4.21	19.04±2.25
Mabozi trench	MBZ-OSL-10	1.66	7.77	1.79	3.42	33.64±2.19	9.83±1.17
Wulancun trench	WLC-OSL-08	2.29	9.71	1.59	3.65	13.08±0.78	3.59±0.42
Wulancun trench	WLC-OSL-10	3.35	9.72	1.88	4.33	163.45±11.91	37.76±4.67
Wulancun trench	WLC-OSL-09	2.23	9.55	1.34	3.35	31.41±2.71	9.38±1.24

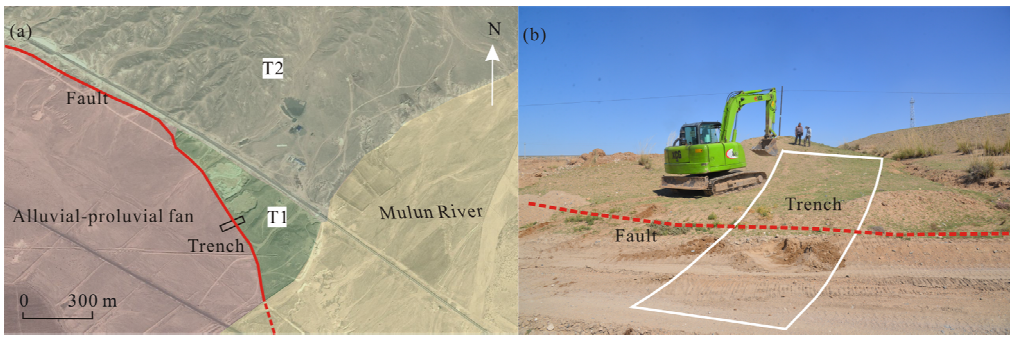

Figure 3. Sketch map of the Dongshuiquan trench. (a) Trench site on the geological map; (b) trench site on the topographic photo.

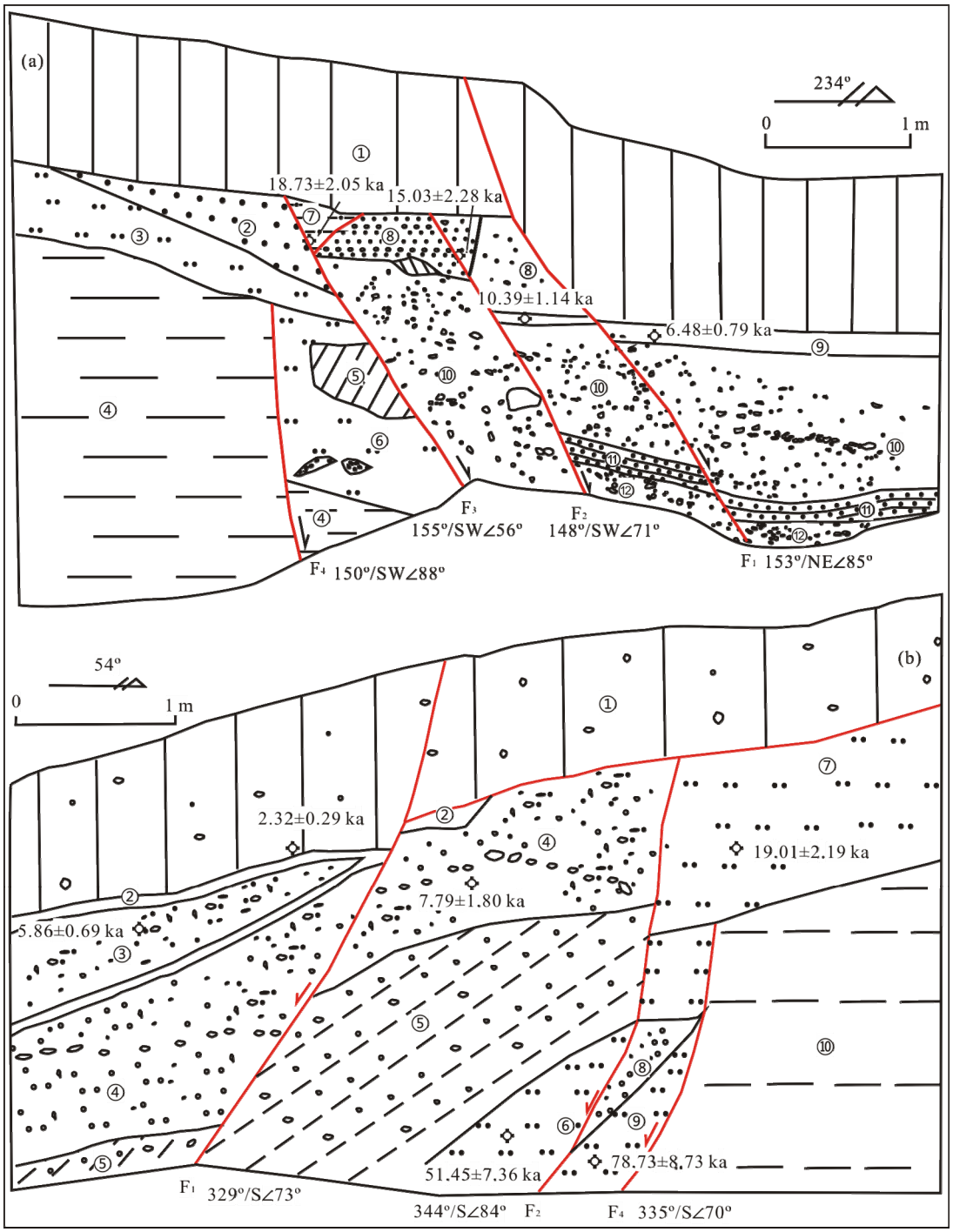

Figure 4. (a) Sketch map of the east wall: ① brown loose fine sand layer containing gravel; ② unstratified yellow-green fine sand layer, ③ gray white silty sand layer containing calcareous cement at the bottom; ④ brown clay layer, more than 3 m thick (full depth unknown); ⑤ yellow-green clay layer containing hard cement; ⑥ thin fine gravel layer lens 10–15 m thick, with a maximum gravel size of 3 cm; ⑦ gray white sandy soil fault collapse wedge layer; ⑧ brown fine sand layer containing 5% well-sorted and well-rounded gravel with a 5 cm maximum gravel size; ⑨ gray black cemented sand soil layer as paleosol layer; ⑩ gray-yellow fine gravel layer containing silt and most of the gravel equal to 0.1–0.5 cm, with the gravel size increasing to 3–5 cm at the bottom of the layer and occasionally at a maximum gravel size of more than 20 cm; ⑪ gray stratified fine gravel layer, with a 0.5–0.8 cm gravel size; ⑫ gravel layer that is well sorted and not well rounded, with a 5–10 cm gravel size. (b) Sketch map of the west wall: ① brown top cover soil layer containing gravel; ② gray-black dark loessial soil layer containing gravel; ③ soil layer containing 30% gravel with a 4 cm maximum gravel size; ④ poorly sorted, generally rounded, unstratified gravel layer, with an 8 cm maximum gravel size; ⑤ ordinarily sorted subangular gravel layer including inclined beddings, with an 8 cm maximum gravel size, full depth unknown; ⑥ ordinarily sorted subangular gravel layer including horizontal bedding, with a 5 cm maximum gravel size; ⑦ yellow silt layer without obvious bedding; ⑧ gravel layer containing 20% sand without obvious bedding; ⑨ yellow silt layer without obvious bedding and with a 1 cm thick horizontal calcareous cement layer in the middle.

west and east walls of the Dongshuiquan trench reveal 4 faults (Figs. 4a and 4b). Based on the relationship between the faults and the units, we know that the F1, F2 and F4 are revealed at both the west and east walls, the F3 is only revealed at the east wall. We analyzed the paleoseismic events according to the characteristics of the sedimentary formations, strata contact relationships and strata-fault contact relationships.

Event 1 occurred when F4 disrupted the stratum ④, and it was covered by stratum ③ on the east wall and disrupted stratum ⑩ on the west wall. The dating age of layer ⑦ at the bottom of the west wall is 19.01±2.19 ka BP. Layer ⑦ covered the F4 on the west wall. Therefore, Event 1 occurred before 19.01±2.19 ka BP and is close to this dating age.

Event 2 caused the F3 to disrupt the strata beneath layer ① and formed the fault collapse wedge layer ⑦ on the east wall. Event 2 occurred approximately18.73±2.05 ka BP.

Event 3 caused the F2 to disrupt the strata beneath layer ① and formed the fault collapse wedge in layer ⑧ on the east wall. Event 3 occurred approximately15.03±2.28 ka BP.

Event 4 caused the F1 to disrupt the top layer ① on the east wall. The dating age of the bottom of layer ① is 6.48±0.79 ka BP. The F1 ruptured the newer unit than the F2. So there must be more events after Event 3. The fault collapse wedge on the west wall defines a new event which occurred 2.32±0.29 ka BP. The bottom layer ① on the east wall has been cut by the F1 and the vertical displacement is twice as much as the displacement of the bottom layer ① in the west wall which is produced by the Event 5. Therefore, there must be the Event 4 which occurred after 6.48± 0.79 ka BP before Event 5. This event is also recorded on the west wall (Fig. 4b). The F1 disrupted layer ② and turned it into 2 layers separated by layer ③ in the middle on the hanging wall of the west wall. We believe that the dark loessial soil layer ② was in a stable formation process until Event 3 interrupted the formation process and cleaved it into two layers separated by layer ③ in the middle on the hanging wall. The dating age of layer ③ is 5.86±0.69 ka BP, which represents the probable occurrence time of Event 4. So the Event 4 occurred approximately at 5.86±0.69 ka BP.

Event 5 caused the F1 to disrupt the top layer ① and form the fault collapse wedge on the west wall, the dating age of which is 2.32±0.29 ka BP, which represents the occurrence time of Event 5.

The time interval between Event 2 and Event 3 is approximately 3 700 a, and the time interval between Event 4 and Event 5 is approximately 3 540 a. We think the seismicity of this segment conforms to the characteristic earthquake model, the recurrence interval of which is approximately 3 620 a. However, the time interval between Event 3 and Event 4 is approximately 9 170 a, and we believe that an intervening event, which likely occurred at approximately 10.45 ka BP, has been missed. Given this assumption, the Dongshuiquan trench reveals 6 events in total, with a 4 100 a recurrence interval, the latest of which occurred at 2.32±0.29 ka BP. This result revealed Event 1, Event 2, Event 3 and Event 5, involving more events than the previous study. The 1 438 a recurrence interval from the previous study (Chen et al., 2003b) seems short compared with the other three segments of the fault. We think that the 4 100 a recurrence interval from this trench is consistent with the results of the other three segments of the fault and reasonable.

2.2 Mabozi Trench (TC5)

The Mabozi trench is located on the front margin of T1, which is in the 95° direction north of Mabozi Village. The trench is 15 m in length, 5 m in width and 6 m in depth (Figs. 5a and 5b). Six southward-dipping normal faults and one antithetic normal fault have been revealed on the east wall of the Mabozi trench (Fig. 5c). The dip of the southward-dipping normal faults is from 155° to 195°. The dip angles are from 46° to 58°. The dip and dip angle of the antithetic normal fault are 20° and 83°, respectively. There is a complex fracture zone enclosed by the faults F2, F3, F4. The trench revealed several paleoseismic events since the Late Pleistocene and 3 events since 30 ka ago according to the characteristics of strata contact relationship, strata-fault contact relationship and the seismotectonic wedge.

Event 1 occurred after the formation of layer ⑭ and before the formation of layer ⑰. Layer ⑰ was squeezed into the fault zone when the event occurred, and it was disturbed strongly by the faulting. The vertical seismic displacement is more than 50 cm. The occurrence time of this event is approximately 29.07±3.85 ka BP.

Event 2 occurred after the deposition of layer ② and formed the antithetic normal fault F5 disrupted layer ② and the layers below. The layers ⑫, ⑬, ⑭ and ⑮ on the hanging wall have been displaced slightly by the faulting. The vertical seismic displacement is approximately 50 cm. This event occurred after 9.83±1.17 ka BP.

Event 3 caused F4 to disrupt all layers up to the surface. The dating age of the layer ① bottom is 3.9±0.46 ka BP. The thickness of layer ② is largely different at both sides of the F4. The vertical seismic displacement is more than 2 m. The latest event occurred after 3.9±0.46 ka BP.

The trench revealed several paleoseismic events since the Late Pleistocene and Event 2 and Event 3 since the Holocene. The latest event occurred after 3.9±0.46 ka BP.

2.3 Wulancun Trench (TC6)

Three terraces have developed across the outlet stream of the Meiyaogou River, and they are cut by the Sertengshan piedmont fault. We dug 3 trenches individually on the front margins of the 3 terraces. The Wulancun trench is located in the front margin of the T2 terrace, which is 16 m in length, 5 m in width and 6 m in depth (Figs. 6a and 6b). The two walls of the trench revealed similar stratigraphic sequences. Sand liquefaction is found at the bottom of the west wall of the trench (Fig. 6c).

A main fault was revealed on the east wall of the Wulancun trench, which is at a 212° dip direction and 56° dip angle. Two paleoseismic events are confirmed according to the characteristics of the sedimentary formations, strata contact relationship and strata-fault contact relationship.

Event 1 occurred after the formation of layer ⑰ and formed the fault collapse wedge composed of layers ⑱ and ⑲, which is 70 cm high. This event produced a 1.4 m vertical displacement assuming that the height of the fault collapse wedge is usually half of the true vertical displacement. The dating age of the collapse wedge is 37.76±4.67 ka BP, which is much older than the 9.38±1.24 ka age of layer ⑰. This contradiction in ages likely resulted from the formation process of the collapse wedge, which was too fast to fully expose the sample.

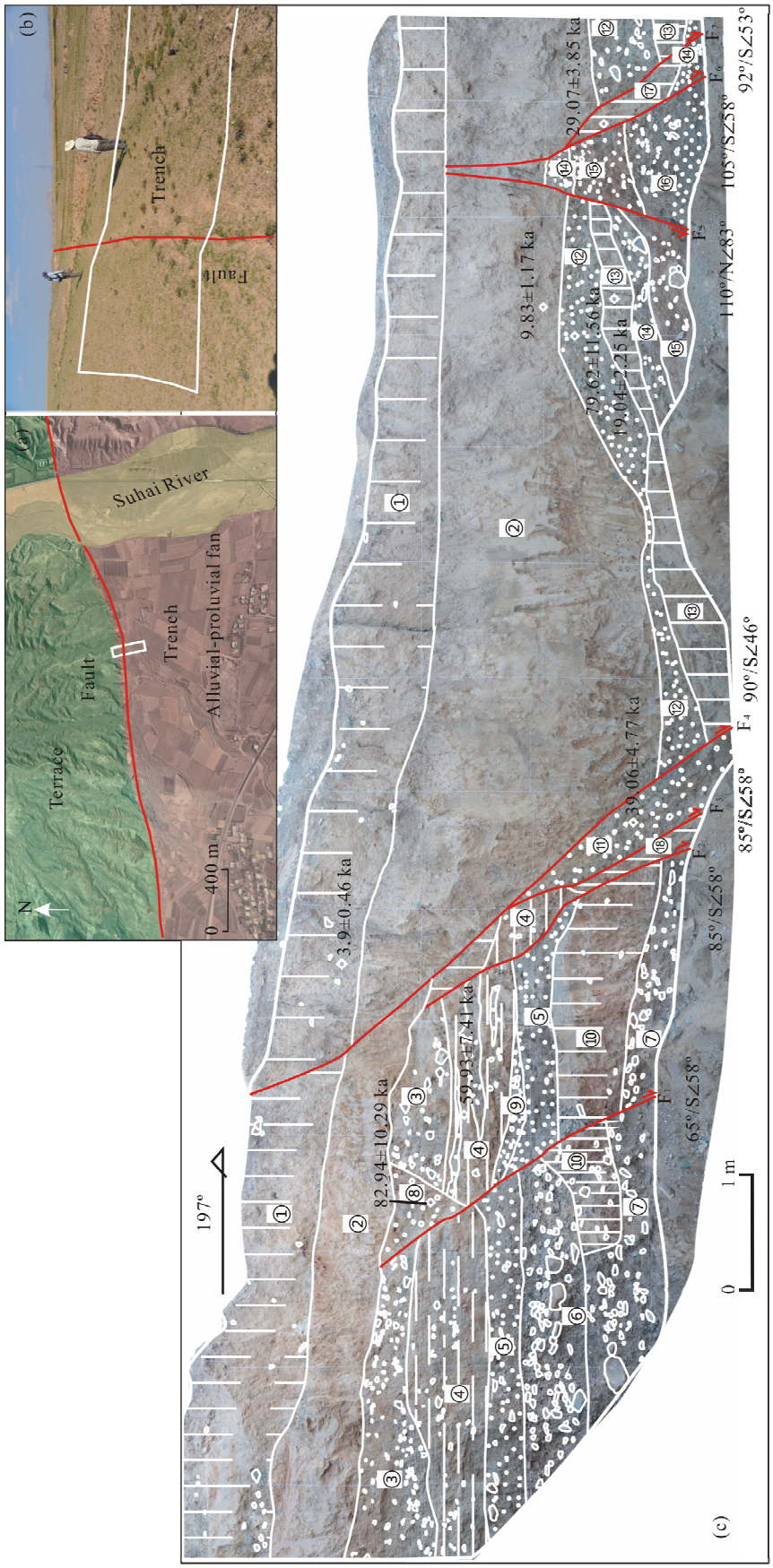

Figure 5. Map of the Mabozi trench and its interpretation. (a) Trench site on the geological map. (b) Trench site on the topographic photo. (c) Sketch map of the east wall: ① Gray black topsoil containing plant roots; ② yellow loess layer containing occasional gravel without joint; ③ poorly sorted, well-rounded gravel layer without obvious bedding containing big size gravel occasionally with the 5–7 cm maximum gravel size. The layer is cut by F1 and F2. ④Gravel layer interbedded with mud including horizontal bedding, disrupted by F1 with the 30 cm coseismic displacement; ⑤ well-rounded, poorly sorted gravel layer, disrupted by F1 with the 30–40 cm coseismic displacement; ⑥ poorly sorted subangular boulder layer with a 15 cm maximum gravel size; ⑦ poorly sorted subangular gravel layer with a 20 cm maximum gravel size, full depth unknown; ⑧ colluvial wedge containing gravel and sands; ⑨ unstratified subangular gravel colluvial wedge with a 5 cm maximum gravel size; ⑩ poorly sorted, poorly rounded gravel layer containing red soil and disrupted by F1 with the 30 cm coseismic displacement; ⑪ poorly sorted, unstratified gray brown gravel in the fracture zone, containing loess and sands, with a 4 cm maximum gravel size; ⑫ gray brown gravel layer, containing locss, with a 4 cm maximum gravel size; ⑬ unstratified locss layer, full depth unknown; ⑭ gray sand-gravel layer with subangular, poorly sorted, poorly rounded gravel; ⑮ unstratified poorly sorted, rusty red sand-gravel layer disrupted by the F5 with a 70 cm coseismic displacement, and the gravel is subangular with a 3 cm maximum gravel size; ⑯ gravel layer with upper and under parts; the upper part is unstratified and the gravel is subangular, poorly sorted or poorly rounded with a 3 cm maximum gravel size. The under part has horizontal bedding and the gravel is well sorted and well rounded with a 4 cm maximum gravel size; and ⑰ loess layer between the F6 and F7 with unstratified with occasional gravel.

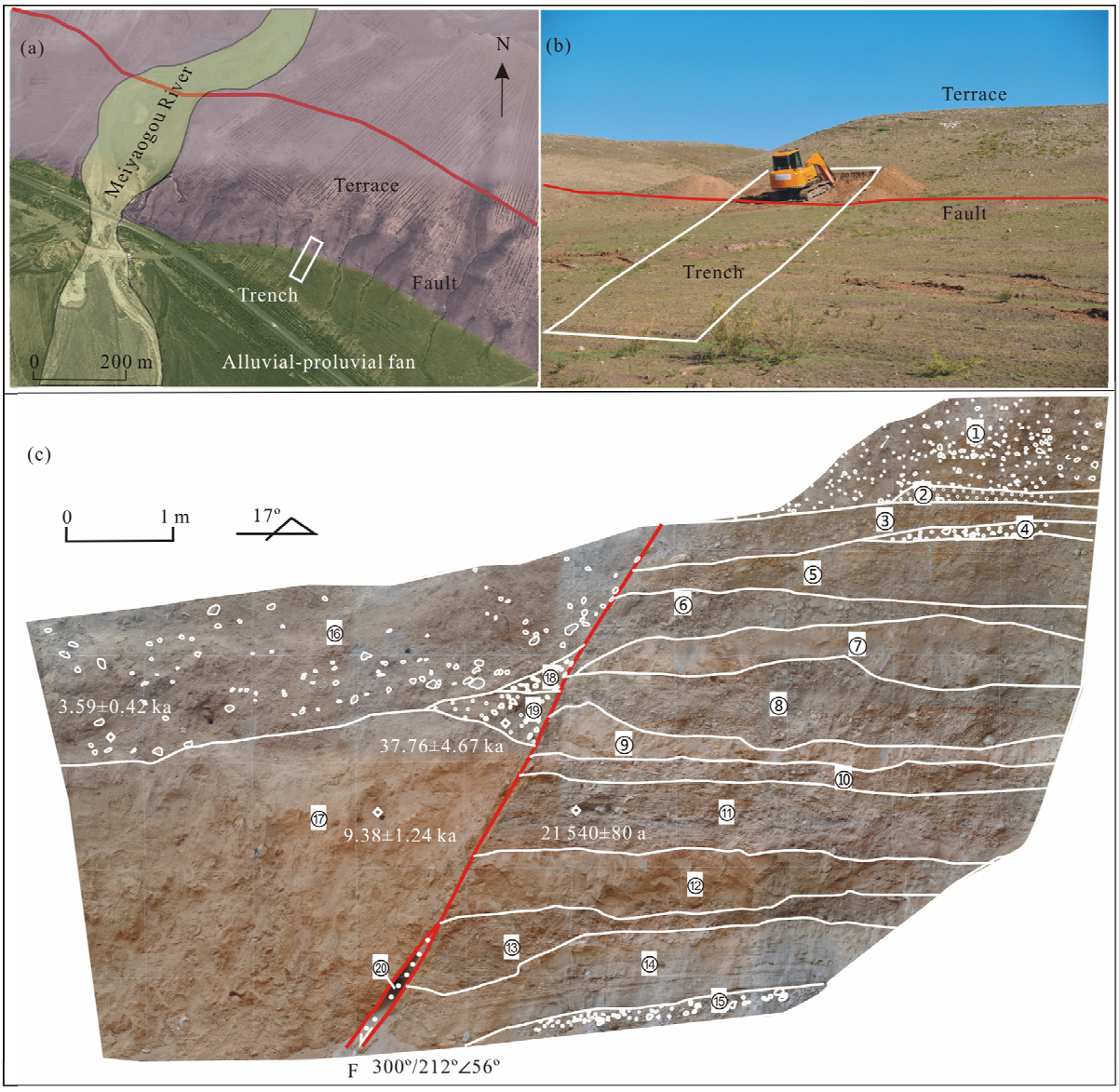

Figure 6. Map of the Wulancun trench and its interpretation. (a) Trench site on the geological map. (b) Trench site on the topographic photo. (c) Sketch map of the west wall: ① Poorly sorted, poorly rounded sand-gravel layer including horizontal bedding, with a 10 cm maximum gravel size; ② 20 cm thin fine sand layer; ③ barely sorted or rounded gravel layer with an 8 cm maximum gravel size; ④ thin medium and fine-grained sand layer, including horizontal bedding; ⑤ poorly rounded, average-sorted pebble gravel layer including horizontal bedding; ⑥ barely sorted or rounded gravel layer with an 8 cm maximum gravel size; ⑦ 20 cm thick loess layer, with a 50 cm maximum thickness; ⑧ average-sorted, poorly rounded gravel layer, including inclined beddings with the 5 cm maximum gravel. There is a yellow 2–4 cm thick fine gravel layer, including horizontal bedding in the middle; ⑨ loess layer; ⑩ barely sorted, poorly rounded gravel layer with a 4 cm maximum gravel size; ⑪ well-sorted, average-rounded pebble gravel layer containing sands, including horizontal bedding, with a 5 cm maximum gravel size, there is a 2–5 cm horizontal thick gravel layer containing carbon; ⑫ brown coarse sand-gravel layer; ⑬ average-sorted brown gravel layer including horizontal bedding; ⑭ gray white well-sorted pebble gravel layer including horizontal bedding, with a 5 cm thick boulder layer and a 40 cm maximum gravel size; ⑮ unstratified well-rounded gravel layer, full depth unknown; ⑯ gravel-soil layer containing plant roots; ⑰ unstratified loess containing angular gravel with a 6 cm maximum gravel size; ⑱ poorly sorted sand-gravel layer; ⑲ under part of the fault collapse wedge containing silty-fine sands and gravel; ⑳ the upper part of the fault collapse wedge containing medium-fine sands

Therefore, the collapse wedge represents one event that occurred after 9.38±1.24 ka BP.

After the collapse wedge was produced by Event 1, layer ⑯ covered the fault and the collapse wedge, and the fault then moved again when Event 2 occurred and disrupted the collapse wedge and the layer ⑯ above. The dating age of the bottom of layer ⑯ is 3.59±0.42 ka BP; therefore, Event 2 occurred after 3.59±0.42 ka BP.

This trench revealed two Holocene paleoseismic events on the segment and constrained the latest event to after 3.59±0.42 ka BP. This result contributes further evidence in support of prior findings.

3 DISCUSSION

3.1 Paleoseismic Events on the East Segments

As many studies have shown, a single trench cannot com-

pletely reveal the paleoseismic events on one active fault segment, although trenches located at different sites on the fault segment may be able to reveal the events completely. Trenches on the same active fault segment can reveal the same events or different events. Certain trenches reveal the lower time limit of the event, whereas others reveal the upper time limit and the time interval. Different trenches on the same fault segment can be comprehensively analyzed to determine the definite paleoseismic events of the active fault segment (Ran et al., 2002; Mao and Zhang, 1995). This paper combines 5 events from the Dongfengcun trench (TC1) (Yang et al., 2002), 6 events from the Dongshuiquan trench (TC2) on the Kuoluebulong segment; and 4 events from the Hongmingcun trench (TC3), 4 events from the Wulanhudong trench (TC4) (Chen et al., 2003b), 3 events from the Mabozi trench (TC5) and 2 events from the Wulancun trench (TC6) in the Dashetai segment and comprehensively analyses these trenches to obtain the exact paleoearthquake sequence of both segments since 30 ka ago (Fig. 7).

According to the comprehensive analysis of the trenches, we obtain the paleoseismic events on both segments of the Sertengshan piedmont fault since 30 ka ago. Six events occurred on the Kuoluebulong segment since 30 ka ago at 19.01–37.56, 18.73, 15.03, 10.96, 5.77–6.48 and 2.32 ka BP. Six events occurred on the Dashetai segment since 30 ka ago at 29.07, 19.12–28.23, 13.92–15.22, 9.38–9.83, 6.08–8.36, and 3.59 ka BP (Table 2).

The latest 5 events on the Kuoluebulong segment display a quasiperiodic recurrence with a mean recurrence interval of 4 100 a, and the 5 events are complete. The oldest event, which occurred from 19.01 to 37.56 ka BP, cannot be defined exactly because of its large time interval and requires further study. The 6 events on the Dashetai segment do not show an obvious quasiperiodic recurrence feature. However, the other events (except the event which occurred 19.12–28.23 ka BP) still occurred quasiperiodically, with a mean recurrence interval of 4 900 a, which is close to the above mean recurrence interval of 4 100 a of the Kuoluebulong segment. In addition, the mean occurrence time of each event of the 6 events on both segments are similar. Therefore, we believe that the paleoseismic events might conform to the cascade rupturing model between the two segments of the Sertengshan piedmont fault.

3.2 Latest Event

On November 11, 7 BC (September Bingchen, the second year of Suihe, Han Dynasty), an *M* 8.0 earthquake occurred as recorded by the chronology of Chinese earthquakes (Seismic History Work Committee of the Chinese Academy of Sciences, 1956), Compilation of Historical Materials of Chinese Earthquake

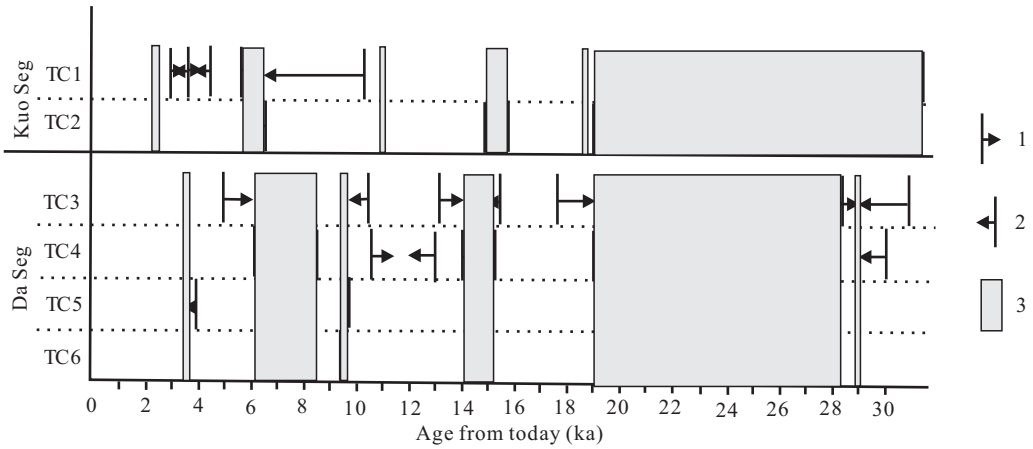

Figure 7. Paleoseismic events on the east segments of the Sertengshan piedmont fault up to 30 ka ago. 1. Upper limit era of paleoseismic events; 2. lower limit era of paleoseismic events; and 3. ultimately determined era scope of paleoseismic events. TC1. Dongfengcun trench; TC2. Dongshuiquan trench; TC3. Hongmingcun trench; TC4. Wulanhudong trench; TC5. Mabozi trench; TC6. Wulancun trench.

Table 2 Paleoseismic events on the east segments of the Sertengshan piedmont fault from approximately 30 ka ago

Segment	Event	Event occurrence time interval (ka BP)	Event mean occurrence time (ka BP)	Time interval	Mean recurrence interval (a)
Kuoluebulong	1	2.32	2.32		4 102
segment	2	5.77–6.48	6.13	3 810	
	3	10.96	10.96	4 830	
	4	15.03	15.03	4 070	
	5	18.73	18.73	3 700	
	6	19.01–37.56	28.29	9 560	
Dashetai	1	3.59	3.59		4 093
segment	2	6.08–8.36	7.27	3 680	
	3	9.38–9.83	9.6	2 330	
	4	13.92–15.22	14.57	4 970	
	5	19.12–28.23	23.68	9 110	
	6	29.07	29.07	5 390	

(Xie et al., 1983) and other important historical documents in China, such as Han Shu (Volume 27) Wuxingzhi (Anonymous, 1986), Imperial Readings of the Taiping Era (Li, 1960), Comprehensive Mirror for Aid in Government (Si, 1992), the Compendium of Works of Past and Present (Jiang, 1934), the list of natural and man-made disaster of China's past dynasties (Chen, 1986), the general history of China's disaster (Qin and Han dynasties volume) (Yuan, 2009), Jinzhou Records (Shen, 1968), Yananfu Records (Hong, 1802), Qingyangfu Records (Liang, 1992), Zhengning County Records (Zhe, 2005). This earthquake affected a large area, including Gansu, Ningxia, Shanxi, Inner Mongolia, Hebei and Beijing (Cao, 1987), and it destroyed more than 30 cities in the north of Xi'an City and killed more than 400 (Xun, 1696) or 415 people (Ban, 1962). This destructive earthquake happened more than 2 000 a ago and had a wide range of influence. There is disagreement regarding the epicenter location of the historical earthquake.

According to the historical records and the isoseismal map (Institute of Geophysics, SSB, Institute of Historical Geography of Fudan University, 1990), the epicenter is in the north margin of the Ordos Block. Sun (1985) regards the Yellow River fault-bend basin as the epicenter's location. Nie (2013) concluded that the epicenter is in Baotou City, which is located on the Daqingshan active piedmont fault.

The historical *M* 8.0 earthquake, which occurred on November 11, 7 BC, was unlikely to have been located on the northwest of the Ordos Block because all the earthquakes during that period have been recorded completely except this particular event. Moreover, the earthquake likely did not occur on the northeast of the Ordos block, including north of Hebei Province and east of Liaoning Province, because this earthquake was not recorded while others were recorded in detail. Therefore, the earthquake likely occurred in the Yellow River fault-bend basin.

The Sertengshan (F1 in Fig. 1), Wulashan and Daqingshan piedmont faults (F2, F3 in Fig. 1) compose the northern fracture zone of the Yellow River fault-bend basin and control the basin's formation and development (He and Ma, 2015). The west segments of the Sertengshan piedmont fault and Wulashan fault have been studied extensively and the results show that the latest events on the two faults occurred 4 190 a BP (Chen et al., 2003a) and 4 130 a BP (Ran et al., 2003), respectively, which do not correspond to the historical *M* 8.0 earthquake, which occurred on November 11, 7 BC. The latest paleoseismic event on the Daqingshan piedmont fault is the A.D. 849 earthquake, which was also an *M* 8.0 event and occurred to the east of Baotou City. The A.D. 849 earthquake's epicenter location is reliable based on a number of studies. If both the 7 BC and A.D. 849 earthquakes happened on the Daqingshan fault and around Baotou City, then the interval between the earthquakes would be 856 a, and this value is too short to match the recurrence interval of the characteristic earthquakes on the Daqingshan fault, which is more than 2 000 a based on previous studies (He and Ma, 2015; Ran et al., 2003). Therefore, the 7 BC historical earthquake could not have happened on the Daqingshan fault. The latest event at 2 320 a BP from our study on the Kuoluebulong segment of the Sertengshan piedmont fault is close to the 7 BC earthquake that happened 2 023 a ago.

According to the analysis above, we conclude that the 7 BC earthquake occurred on the Kuoluebulong segment of the Sertengshan piedmont fault, and it represents the latest event on the Kuoluebulong segment of the Sertengshan piedmont fault as described in this study.

4 CONCLUSIONS

Based on the study of the characteristics of the geometrical distribution, tectonic activity and geomorphological features as well as the paleoearthquake and segment boundary features of the Sertengshan piedmont fault, we divided the fault into 4 segments: Langshankou (Dongwugai-Wayaotan) and Hongqicun (Dahoudian-Wubulangkou) segments in the EW direction and the Kuoluebulong (Wubulangkou-Wayaotan) and Dashetai (Wayaotan-Tailiang) segments in the NW direction.

Three trenches analyzed in this paper and three trenches analyzed in previous studies were comprehensively investigated, and the results reveal that 6 paleoseismic events have occurred on the Kuoluebulong segment since approximately 30 ka BP in succession as follows: 19.01–37.56, 18.73, 15.03, 10.96, 5.77–6.48, and 2.32 ka BP. Six paleoseismic events have occurred on the Dashetai segment since approximately 30 ka BP in succession as follows: 29.07, 19.12–28.23, 13.92–15.22, 9.38–9.83, 6.08–8.36, and 3.59 ka BP.

The events on the Kuoluebulong segment display quasiperiodic recurrence with a mean recurrence interval of 4 100 a. The events on the Dashetai segment do not display obvious quasiperiodic recurrence. However, except for the event that occurred from19.12–28.23 ka BP, the other events show a quasiperiodic recurrence feature with a mean recurrence interval of 4 900 a. The mean occurrence time of each event of the 6 events on both segments is similar. Therefore, we believe that the paleoseismic events might conform to the cascade rupturing model between the two segments of the Sertengshan piedmont fault.

The latest event on the Kuoluebulong segment of the Sertengshan piedmont fault is the historical *M* 8.0 earthquake that occurred on November 11, 7 BC, which was recorded by a large number of Chinese historical texts.

ACKNOWLEDGMENTS

This study was supported by the Institute of Crustal Dynamics, China Earthquake Administration (No. ZDJ2016-11), the National Natural Science Foundation of China (No. 41602221) and the 1 : 50 000 Geological Mapping of the Sertengshan Piedmont Fault (No. 201408023). The OSL samples were analyzed by Dr. Junxiang Zhao at the Key Laboratory of Crustal Dynamics, Institute of Crustal Dynamics, China Earthquake Administration. We thank the anonymous reviewers for their helpful comments on the manuscript. The final publication is available at Springer via https://doi.org/10.1007/s12583-017-0937-z

REFERENCES CITED

Aitken, M. J., 1998. An Introduction to Optical Dating. Oxford University Press, Oxford

Anonymous, 1986. Han Shu (Volume 27) Wuxingzhi. Shanhai Ancient Literature Press, Shanghai. 507 (in Chinese)

Ban, G., 1962. Han Shu (Volume 27) Wuxingzhi. Zhonghua Book Company, Beijing. 1454–1455 (in Chinese)

Cao, Z. X., 1987. Historical Earthquake References of Beijing Area. For-

bidden City Press, Beijing. 1 (in Chinese)

Chen, G. Y., 1986. The List of Natural and Man-Made Disaster of China's Past Dynasties. Shanghai Bookstore Publishing House, Shanghai. 57 (in Chinese)

Chen, L. C., Ran, Y. K., Chang, Z. P., 2003b. Characteristics of Late Quaternary Faulting and Paleoseismic Events on the East of Delingshan Segment of the Sertengshan Piedmont Fault. *Seismology and Geology*, 25: 556–565 (in Chinese with English Abstract)

Chen, L. C., Ran, Y. K., Yang, X. P., 2003a. Late Quarternary Activity and Segmentation Model of the Sertengshan Piedmong Fault. *Earthquake Research in China*, 19(3): 255–265 (in Chinese with English Abstract)

Deng, Q. D., Zhang, P. Z., 1995. Principles and Methods for Segmentation of Active Faults. In: Institute of Geology, State Seismlolgical Bureau, ed., Research on Recent Crustal Movement (6). Seismological Press, Beijing. 196–207 (in Chinese with English Abstract)

Ding, G. Y., Tian, Q. J., Kong, F. C. et al., 1993. Segmentation of Active Fault: Principle, Method and Application. Seismological Press, Beijing (in Chinese)

Du, W., Jiang, Z. X., Li, Q., et al., 2016. Sedimentary Characterization of the Upper Paleozoic Coal-Bearing Tight Sand Strata, Daniudi Gas Field, Ordos Basin, China. *Journal of Earth Science*, 27(5): 823–834. https://doi.org/10.1007/s12583-016-0705-5

He, Z. T., Ma, B. Q., 2015. Holocene Paleoearthquakes of the Daqingshan Fault Detected from Knickpoint Identification and Alluvial Soil Profile. *Journal of Asian Earth Sciences*, 98: 261–271. https://doi.org/10.13039/501100001809

Hong, H., 1802. Jiaqing Reversed 'Yananfu Records', Vol. 4. Phoenix Publishing House, Hongkong. 27 (in Chinese)

Institute of Geophysics, SSB, Institute of Historical Geography of Fudan University, 1990. Atlas of Historical Earthquakes in China. China Cartographic Publishing House, Beijing (in Chinese)

Jiang, T. X., 1934. The Compendium of Works of Past and Present. Zhonghua Book Company, Beijing (in Chinese)

Jiang, W. L., Wang, X., Tian, T., et al., 2014. Detailed Crustal Structure of the North China and Its Implication for Seismicity. *Journal of Asian Earth Sciences*, 81: 53–64. https://doi.org/10.1016/j.jseaes.2013.11.021

Li, F., 1960. Imperial Readings of the Taiping Era. Zhonghua Book Company, Beijing (in Chinese)

Liang, M. H., 1992. Qingyangfu Records, Vol. 18. Zhonghua Book Company, Beijing. 529 (in Chinese)

Lu, Y. C., Wang, X. L., Wintle, A. G., 2007. A New OSL Chronology for Dust Accumulation in the last 130 000 yr for the Chinese Loess Plateau. *Quaternary Research*, 67(1): 152–160. https://doi.org/10.1016/j.yqres.2006.08.003

Mao, F. Y., Zhang, P. Z., 1995. Progressive Constraining Method in Paleoseismic Study and Paleoearthquakes along the Major Active Faults in Northern Xinjinag, In: Institute of Geology, SSB, eds., Research on Acvive Fault (4). Seismological Press, Beijing. 153–164 (in Chinese with English Abstract)

Murray, A. S., Wintle, A. G., 2000. Luminescence Dating of Quartz Using an Improved Single-Aliquot Regenerative-Dose Protocol. *Radiation Measurements*, 32(1): 57–73. https://doi.org/10.1016/s1350-4487(99)00253-x

Murray, A. S., Wintle, A. G., 2003. The Single Aliquot Regenerative Dose Protocol: Potential for Improvements in Reliability. *Radiation Measurements*, 37(4/5): 377–381. https://doi.org/10.1016/s1350-4487(03)00053-2

Nie, Z. S., 2013. Preliminary Investigation on the Historical *M* 8 Earthquake Occurred in 7 BC at Baotou, Inner Mongolia. *Acta Seismologica Sinica*, 35: 584–603 (in Chinese with English Abstract)

Nulay, P., Chonglakmani, C., Feng, Q. L., 2016. Petrography, Geochemistry and U-Pb Detrital Zircon Dating of the Clastic Phu Khat Formation in the Nakhon Thai Region, Thailand: Implications for Provenance and Geotectonic Setting. *Journal of Earth Science*, 27(3): 329–349. https://doi.org/10.1007/s12583-016-0667-7

Ran, Y. K., Chen, L. C., Yang, X. P., et al., 2003. Recurrence Characteristics of Late Quaternary Strong Earthquakes on the Major Faults along the Northern Border of Ordos Block. *Science in China Series D: Earth Sciences*, 46: 189–200 (in Chinese)

Ran, Y. K., Zhang, P. Z., Hu, B., et al., 2002. Paleoseismic Activity on the Hohhot Segment of Daqingshan Piedmont Fault in the Late Quaternary History. *Earthquake Research in China*, 18: 15–27 (in Chinese with English Abstract)

Research Group on 'Active Fault System around Ordos Massif', SSB, (1988). Active Fault System around Ordos Massif. Seismological Press, Beijing. 39–76 (in Chinese)

Seismic History Work Committee of the Chinese Academy of Sciences, 1956. Chronology of Chinese Earthquakes. Science Press, Bejjing. 1, 181–182, 303, 359, 440 (in Chinese)

Shen, R., 1968. Jinzhou Records 1(2). Taiwan Students Bookstore, Taipei. 323 (in Chinese)

Si, M. G., 1992. Comprehensive Mirror for Aid in Government. Zhonghua Book Company, Beijing. 1063 (in Chinese)

Sun, J. L., 1985. The Probability of Strong Earthquakes in the Northern Margin of the Ordos Block. *Northwestern Seismological Journal*, (S1): 13–23 (in Chinese with English Abstract)

Wheeler, R. L., 1989. Persistent Segment Boundaries on Basin-Range Normal Faults. In: Schwartz, D. P., Sibson, R. H., eds., Proceedings of the of Workshop XL V-Fault Segmentation and Controls of Rupture Initiation and Termination. *U.S. Geol. Surv. Open-file Rep*., 89(315): 432–444

Wu, W. M., Nie, Z. S., Xu, G. L., 1996. Research on the West Segment of the Serteng Piedmont fault. Research on Active Faults (5). Seismological Press, Beijing. 113–123 (in Chinese with English Abstract)

Xie, Y. S., Cai, M. B., Wang, H. A., et al., 1983. Compilation of Historical Materials of Chinese Earthquake (Vol. 1). Science Press, Beijing. 12–13 (in Chinese with English Abstract)

Xun, Y., 1696. Annals of the Han Dynasty China. Kangxi Bingzi Year Block-Printed Edition 2. Beijing (in Chinese)

Yang, X. P., Ran, Y. K., Hu, B., et al., 2002. Active Fault and Paleoearthquakes of the Piedmont Fault (Wujumengkou-Dongfeng Village) for Serteng Mountain, Inner Mongolia. *Earthquake Research in China*, 18: 127–140 (in Chinese with English Abstract)

Yang, X. P., Ran, Y. K., Hu, B., et al., 2003. Paleoseismic Activity on Wujiahe Segment of Serteng Piedmont Fault, Inner Mongolia. *Acta Seismologica Sinica*, 16(1): 67–78. https://doi.org/10.1007/s11589-003-0008-7

Yuan, Z. L., 2009. The General History of China's Disaster (Qin and Han Dynasties Volume). Zhengzhou University Press, Zhengzhou. 82 (in Chinese with English Abstract)

Zhang, P. Z., Deng, Q. D., 1995. Principles and Methods for Segmentation of Active Faults. In: State Seismlolgical Bureau, eds., Institute of Geology. Research on Recent Crustal Movement (6). Seismological Press, Beijing. 208–215 (in Chinese with English Abstract)

Zhang, P. Z., Mao, F. Y., Chang, X. D., 1998. The Criteria for Active Fault Segmentation in Seismic Safety Assessment of Major Engineering. *Seismology and Geology*, 20: 289–301 (in Chinese with English Abstract)

Zhe, Y. L., 2005. Zhengning County Records, Vol. 13. Gansu Culture Press, Lanzhou. 162 (in Chinese with English Abstract)